

# Gas Transport Characteristics of Mixed Matrix Membrane Containing MIL-100 (Fe) Metal-Organic Frameworks and PEBAX Precursors

Vahid Pirouzfard (✉ [v.pirouzfard@iauctb.ac.ir](mailto:v.pirouzfard@iauctb.ac.ir))

Islamic Azad University Central Tehran Branch <https://orcid.org/0000-0002-2862-008X>

Narges Roustaie

Mahmoud Salimi

Chia-Hung Su

---

## Research Article

**Keywords:** Mixed Matrix Membrane, MOF, MIL-100, PEBAX, Selectivity

**Posted Date:** December 13th, 2021

**DOI:** <https://doi.org/10.21203/rs.3.rs-1155966/v1>

**License:**   This work is licensed under a Creative Commons Attribution 4.0 International License.

[Read Full License](#)

---

# Abstract

In this research, the effect of adding MIL-100 (Fe) MOFs on the PEBA membranes has been scrutinized in two grades of 1657 and 2533. Initially, the intended membranes were synthesized by the solution-casting method. Then, the XRD and SEM were applied to deliberate the influence of adding MIL-100 (Fe) to the structure of both types of membranes. In consequence, the separation function of the pair gases of  $\text{CO}_2/\text{CH}_4$ ,  $\text{CO}_2/\text{N}_2$  and  $\text{CO}_2/\text{O}_2$  and their permeability were considered at the pressure of 3.5 bar and temperature of 25°C. Eventually, their function was compared by Robeson diagrams of 1991 and 2008. The comparison results by Robeson diagrams indicated that the PEBA1657/MIL-100 (Fe) and PEBA2533/MIL-100 (Fe) membranes containing 5 wt.% of MOF represent more suitable performance in separating  $\text{CO}_2/\text{CH}_4$  in comparison with the axis of the Robeson diagram. However, their function for separating the aforementioned gases requires more modifications.

## 1. Introduction

These days, membrane technologies have vastly come into consideration for several reasons such as low energy consumption, the low volume of modules, the possibility and availability, without thermal sensitivity, the very negligible pressure drop, low energy loss and low investment costs in comparison with other separation methods [1–6]. Regardless of the fact that membrane technologies have remarkable advantages in comparison with other separation methods, membrane processes are mainly dealt with several problems such as concentration polarization, blockage, not predicting the proper behavior of the membrane, stability, incomplete separation, purification and low permeability [7–13]. Among the aforementioned problems, membranes have been used the least in the gas separation process for the sake of their low permeability and selectivity [14–19]. Thus, it is essential to give priority to make membranes with high simultaneous permeability and selectivity [20, 21]. Based on this concept and their structure, membranes are divided into dense and porous materials. In dense membranes, the difference in the solubility amount or the permeability of the components into the polymeric bed is considered as the main reason for separating the components of a compound by these membranes [22]. In general, these membranes have good selectivity but low permeability. Porous membranes are so similar to the common filters from the function and structure viewpoints [12, 13]. The structure of these membranes is hard and made up of pores that have heterogeneous diffusion. These pores are continuous and they make a canal through the membrane structure [22, 23]. In practice, porous membranes have a high passing fluid, but its selectivity is low. The competition between selectivity and permeability of polymeric and porous membranes is not limited to one certain membrane, but it is true for all the made membranes [19–23].

In 1991, Robeson indicated that the selectivity of all dense membranes is under the line based on their permeability which is known as the upper bound of Robeson [24, 25]. This direct line which features out the ideal selectivity of pair gases due to the permeability algorithm of more permeable gas, indicates the same competition between selectivity and permeability of membranes. Polymeric membranes suffer from a reverse relation between permeability and selectivity [22]. The concept of mixed network

membranes was presented to solve the problem of polymeric membranes. So far, many substances have been used to produce mixed membranes such as carbon molecular sieve [26], zeolites [27], MOFs [28, 29], active carbon [30] and carbon nanotubes (CNTs) [8, 11, 20].

In some researches, the effect of CNTs, alumina and silica nanoparticle, SiO<sub>2</sub>, multiwall carbon nanotubes, Zinc Oxide on different mixed matrix membranes were reviewed and investigated [14–21]. Making these mixed membranes was dealt with several problems such as weak interaction between particle and polymer matrix and weak and heterogeneous diffusion of the particles filling inside the continuous phase of the polymer [20, 21]. On the other hand, particle size, porosity size of the particle, the volume percentage of the dense phase and the chemical properties of the polymer were remarked. Among all types of particles used for the production of mixed membranes, MOFs can work efficiently to remove most of the aforementioned problems of the network for different reasons [28, 29].

The nanostructure of the Metal-Organic compounds has a specific surface and lots of porosities and the size of their Nanopores can be regulated. In fact, they can simultaneously increase the permeability and selectivity of the membrane. The completely organized, regular and homogenous Nanopores are counted as other advantages of these frames because they have made up of the same repeated units [28–30]. This distinguishes these types of substances from carbonic substances and zeolites. This is regarded as a significant factor increasing the selectivity. The remarkable variety of these compounds is caused by the type of ligand and metals. The ligand- metal coordinated bonds and bonds between the donor and receptive molecules and hydrogenic bonds. From another point of view, various polymers have been synthesized and evaluated to achieve a suitable MMM for gaseous separation processes with polymeric base [22, 31, 32]. In polymeric precursors, polymers like PEBAX are commercial thermo-plastics that have been used in different gaseous separations [33, 34]. Kim et al. mulled over the separation properties of the mixed network membrane of the gas which has been made of PEBAX. They dissected the effect of the chemical components of PEBAX co-polymer on the permeability of the polar and non-polar pair gases like CO<sub>2</sub>/N<sub>2</sub>. The results reveal that the permeability of the permeating non-polar gases is reduced as the molecular size of these gases is increased [34].

Regarding the aforementioned items, the effect of adding MOF with the optimized and suitable structure on two suitable and selected grades from PEBAX polymer has been scrutinized in this current research. The XRD and SEM tests have been applied to assess the optimized membranes. The effects of adding MIL-100 (Fe) to the structure of both types of polymers and their interaction has been measured as one of the innovations of this research. Finally, the features were evaluated and the separation of the paired gases of CO<sub>2</sub>/CH<sub>4</sub>, CO<sub>2</sub>/N<sub>2</sub> and CO<sub>2</sub>/O<sub>2</sub> and their permeations were considered.

## 2. Materials And Methods

### 2-1. Polymeric Precursors

Polymers like PEBAX are commercial thermoplastics that have been used in different gaseous separations. Table 1 displays the specifications of the grades 2533 and 1657 of PEBAX polymer [30]. DMF is an organic compound which has been used as a solvent. Its properties are illustrated in Table 2. The cylinders containing pure gases of N<sub>2</sub> and CO<sub>2</sub> have been used as feed to test and assess the membrane permeability.

Table 1  
The properties of the PEBAX polymer grades

Properties	Unit	PEBAX1657	PEBAX2533
contents PE	Wt.%	60	80
Density	g/cm <sup>3</sup>	1.14	1
Melting Point	°C	204	134
Glass transition	°C	-56	-65
Stress in tears	MPa	32	32

Table 2  
DMF solvent properties

Name	Dimethylformamide [(CH <sub>3</sub> ) <sub>2</sub> NCH]
Molecular mass	73.09 g.mol <sup>-1</sup>
Boiling point	153°C
Melting point	60.5°C
Density	948 mg.mL <sup>-1</sup>
Steam pressure	516 Pa
Flash point	58°C

## 2-2. Synthesis of MOF (MIL-100) Fe

The Fe Lewis acid sites are produced by omitting two molecules of H<sub>2</sub>O belonging to the octahedra Fe bases and the partial removal of anions through vacuum activation. Therefore, lots of Fe Lewis acidic sites can be obtained in pores within the MIL-100 (Fe) synthesis by considering the functions of this process. Structural studies indicate that there are remarkable substances for surface absorption which can be utilized in processes requiring surface absorption and desorption [30, 31].

## 2-3. Laboratory Equipment

The magnetic stirrer includes a magnet with a cover that is neutral to all chemicals. There is also a hot plate and a magnetic engine inside the device. When the magnet inside the engine starts rotating, the magnet inside the solution container moves it. So, the temperature and the rotation speed of the magnet inside the solution container can be simply set and controlled. Fig. 1 features out a schematic of a membrane module and magnetic stirrer. The ultrasonic cleaner is a metallic container containing some water. This device is utilized to disperse nanoparticles in liquids and diffuse nanoparticles and degas the membrane solution.

#### 2-4. MMM Preparation Procedures

The solution-casting method was used to make a membrane. Indeed, the suitable thickness in this experiment was considered to be 100 $\mu\text{m}$ . For this purpose, the polymer and nanoparticle were weighed by mixing different percentages of 5, 10 and 15 wt.% of the nanoparticle.

To diffuse the nanoparticle through the solution and have a homogenous composite and pores with the homogenous gap, the beaker containing the nanoparticle and solvent was put in the ultrasonic cleaner for 20 min. After using the ultrasonic cleaner, if the solution is stood still for more than 5 min, the solution is deposited. After the nanoparticle solution was added to the polymer, the flask was put on the hot plate. The thermometer and the pipe connected to the flask and the magnet was dropped into the flask.

To completely disperse the MIL-100 and the intended polymer by rotating the magnet on the stirrer device, the test should be done at the temperature of 110 to 120  $^{\circ}\text{C}$  for 4 hours. After several tests, it was determined that 240 min is needed for complete dissolution and homogenization. The homogenous solution was obtained after 225 min. In the last 15 min, one drop of oil is added to the solution to simply separate the membrane from the plate while it is being stirred. From one hour earlier, the glass plate was washed by distilled water. It was put in the oven at the temperature of 70 $^{\circ}\text{C}$ . It should be noted that homogenous diffusion on the plate should have the same temperature when the membrane solution was poured on the plate.

Now, the composite solution which includes PEBAX (2533 or 1657) polymer the MIL-100 nanoparticle and DMF solvent is slowly poured on the plate and a membrane with a thickness of 100 $\mu\text{m}$  was made. It is exposed to the open air for one or two days so that the solvent is completely evaporated. In the next step, the membrane is put in the oven for 3 hours at the temperature of 70 $^{\circ}\text{C}$  before separating it from the plate. In this stage, the membrane film is ready to separate from the plate.

### 3. Results And Discussion

This section provides details about the characterization of PEBAX2533/MIL-100 (Fe) and PEBAX 1657/MIL-100 (Fe). In consequence, the function of these two membranes in the separation process of  $\text{CO}_2/\text{CH}_4$ ,  $\text{CO}_2/\text{N}_2$  and  $\text{CO}_2/\text{O}_2$  is considered. The XRD and SEM tests were applied to analyze the structure and the surface morphology of the membrane body.

### 3-1. Characterization results of Nanocomposite Membranes

#### 3-1-1. XRD Test

In order to study the structural (crystalline-amorphous) evaluations, some characteristic tests were done on obtained PEBA2533 and PEBA1657 / MIL-100 (Fe) nanocomposite membranes (Fig. 2).

As indicated in Fig. 2.a, the PEBA1657/MIL-100(Fe) membranes have reflected one high wide peak and two high sharp peaks in the 23.85 and 21.45° in the region between angles from 15 to 25°. The wide peak reveals the amorphous structure of the PEO phase of PEBA 1657 polymer which has been formed in this region. The low range long peaks are related to the crystalline phase of PA polymer [31]. Moreover, the 5.56 and 11.05° peaks disclose the presence of MOF in the membrane structure. Their intensity is diminished because of diffusion in the polymer environment. As the amount in the polymer structure is increased to 0.15%, a slightly intensive peak has been shown [32, 33]. Fig. 2.b illustrates the results of XRD for the PEBA 2533/MIL-100 (Fe) for nanocomposite membrane. These membranes include an amorphous phase and a crystalline phase which have been featured out in one wide peak (15 to 25°) and two high sharp peaks (23.85 and 21.69°), respectively. Notably, the wide peak reveals the amorphous structure of the PTMO phase of PEBA2533 polymer which is in this region. High sharp peaks are related to the crystalline phase of PA polymer [32, 33]. Similarly, the peaks 5.56 and 11.05° indicate the presence of MOF in the membrane structure once again. According to the fact that all the nanocomposite membranes made in this research have been synthesized by applying the DMF [33], the boiling point of this solvent is high, it ends to produce membranes with mostly crystalline structure [34]. Thus, the presence of crystalline phases in membrane structure could be predicted. Besides the polymer crystalline structure, it is significant to remark the situation of crystalline peaks and determine the permeation properties in membranes. According to equation Bragg ( $n\lambda = 2d\sin\theta$ ), when the amounts of  $2\theta$  are decreased, the d-spacing increases. The d-spacing is a criterion to measure the molecular spacing of inter-polymeric chain. As the d-spacing gets more, there is more tendency to transmit gas molecules [31, 35]. The d-spacing for grade 2433 will be more than 1657 due to different peaks of PEBA.

#### 3-1-2. SEM results

The SEM test was applied to pore over the effect of adding MIL-100 (Fe) to PEBA2533 and PEBA1657 on the structure and the surface of the nanocomposite membranes. Fig. 3 divulges the results of this experiment. As observed, using PEBA 2533 polymer can lead to produce more porous membranes and this is made by the presence of TMO monomers [36]. Clearly, poly tetra methylene is identified as the fine part of the PEBA2533. Also, this factor makes synthesized membranes have a more porous levels, while polyether amide polymer which is in the structure of PEBA1657 is directed into making bigger pores and more porous structures [37]. This is caused by easier movement and more flexibility of PEBA polymeric chains on the surface [38].

As pointed out, PEBA is an elastomer thermoplastic which is a compound of linear chains of hard polyamide (PA) such as nylon-6 (6PA-) and nylon-12(12PA-). It is set beside the polyether monomers (PE)

and provides flexibility and mechanical power in the final polymer. Besides, poly tetramethyl oxide (PTMEO), which presents excellent properties for gas separation, has been added to the structures of PEBAX2533. According to the results of SEM, it is concluded that the presence of poly tetramethyl oxide (PTMEO) increases the d-spacing which enhances gaseous permeation.

Holistically, it has resulted that the synthesized membranes hold the less dense and suitable structure. As indicated, the effect of adding MIL-100 (Fe) to PEBAX1657 and 2533 polymers on the structure of synthesized membranes have been shown. Observing the SEM images can pave the way to realize that the MOF amount leads to more roughness on the membrane surface. Finally, it improves the absorption process and gas dissolution [39]. Furthermore, it is observed that the lumping amount is increased as this substance is enhanced. Eventually, it might bring about non-selective masses on the surface and the membrane structure [40, 41].

### 3-2. Separation performance of Nanocomposite Membranes

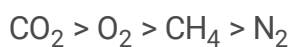
The gaseous separation efficiency of the PEBAX1657 and 2533 nanocomposite membranes were deliberated by adding MIL-100 (Fe) at the pressure of 3.5 bar and temperature of 25°C. In this research, the permeation amount of CO<sub>2</sub>, CH<sub>4</sub>, N<sub>2</sub> and O<sub>2</sub> gases and the pair gas selectivity of these membranes for the CO<sub>2</sub>/CH<sub>4</sub>, CO<sub>2</sub>/N<sub>2</sub> and O<sub>2</sub> were mulled over (Fig. 4). Fig. 4.a features out that the permeation amount of carbon dioxide through the membranes synthesized by PEBAX2533 is more than the ones synthesized by PEBAX1657. The reason of such increase is caused by the presence of the poly tetramethyl oxide monomers which result in the formation of membranes with more porous and flexible membranes.

Additionally, they can pass the gaseous molecules through themselves more easily [42]. Clearly, the polymeric fine parts of tetramethylene oxide (PTMEO), which is in the PEBAX 2533 structure, hasten the transition of gaseous molecules. As the tendency of carbon dioxide to PTMEO is remarkably more than PE for the sake of making hydrogen bonds, such tendency will be high in N<sub>2</sub>, methane and oxygen. As indicated in the XRD analysis, the grade 2533 of PEBAX is more amorphous in comparison with grade 1657. It increases the d-spacing and enlarges the pores of the membrane. Finally, it causes more gas molecules to pass through the membrane. Still, the permeation- dissolution mechanism is identified as the dominant mechanism on passing gases through the dense membranes. The CO<sub>2</sub> molecules tend more to be absorbed on the surface of poly tetramethylene oxide in comparison with polyethylene oxide. This factor intensifies the dissolution of carbon dioxide as well as its passing through the membrane [43]. Notably, it is true for methane gas. As shown, membranes with PEBAX 2533 base have less selectivity than PEBAX1657. It is indicated that the permeation amount of carbon dioxide has been increased in both membranes through adding MIL-100 (Fe) to the membrane. This increase is related to the free fraction volume (FFV) developed by making a pore around MOF diffused nanoparticles [44]. Moreover, the synthesized membranes have more tendency to polar gases like carbon dioxide by adding MIL-100 (Fe) to PEBAX polymer because of having OH polar groups [45]. The FFV enhancement and the increase of OH groups are responsible for the continual permeation increase of this gas and the improvement of the amount of MIL-100(Fe).

The SEM images show that the increase of MOF amount directs into lumping more nanoparticles. At last, more non-selective surfaces and sections are made on the structure of the membranes. As observed, this factor affects the total selectivity of the membrane and its operation. Since PEBA1657 polymer is less flexible and the size of pores are small in the synthesized by this polymer, the passing rate of CH<sub>4</sub>, N<sub>2</sub> and O<sub>2</sub> gases is influenced and reduced. For this reason, better selectivity in membranes PEBA1657/MIL-100 (Fe) was observed in comparison with PEBA2533/MIL-100 (Fe). Fig. 5 reveals that most of the selectivity numbers are related to the pair gases of CO<sub>2</sub>/N<sub>2</sub>, CO<sub>2</sub>/O<sub>2</sub> and CO<sub>2</sub>/CH<sub>4</sub>, respectively. Evidently, it is inferred that the least amount of gaseous permeation is related to N<sub>2</sub> gas, methane gas and carbon dioxide, correspondingly.

As aforementioned, the permeation- dissolution mechanism is the dominant mechanism on passing gases through dense membranes such as gaseous ones. Based on this theory, the gaseous molecules permeate into the membrane and pass through it because they tend to the membrane surface (determining the dissolution coefficients) and they are condensate by the critical temperature [39]. Accordingly, the molecular polar bond among the gases considerably influences the surface dissolution stage. In fact, the molecules of carbon dioxide will have the highest condensation while they are in touch with the polymeric structure of the membrane. As a result, it leads to more permeation in comparison with other gases tested in this research [38, 46].

The enhancement of permeability in PEBA/MIL-100 (Fe) may have resulted from the mixed effects of permeation-dissolution and the molecular screening mechanism and it cannot be explained only by one of the mechanisms. Adding MOF can make a remarkable change in the permeation of carbon dioxide which can be resulted from the ideal selectivity of CO<sub>2</sub>/N<sub>2</sub>, CO<sub>2</sub>/CH<sub>4</sub> and CO<sub>2</sub>/O<sub>2</sub> pair gases. This might be caused by passing more carbon dioxide through the pores of MIL-100 (Fe) which can remarkably prevent the permeation of bigger molecules through the MOF pores [47]. From another point of view, although methane gas is a non-polar molecule, it has polar bonds tending these molecules to the fine PEBA polymer threads. As a result, it ends to more permeation of this gas in comparison with oxygen and N<sub>2</sub> [42]. The next influential factor is the kinetic diameter of gases which determines their amount and permeation coefficient. Since the kinetic diameter of carbon dioxide (3.3A) is less than methane (3.8 A), N<sub>2</sub> (3.64 A) and oxygen (3.46 A), it will have a higher permeation coefficient. Likewise, O<sub>2</sub> and N<sub>2</sub> molecules are non-polar with non-polar bonds. Nonetheless, oxygen has not only a smaller kinetic diameter, but also it has reflected more dissolution in the membrane by making a hydrogen bond with OH groups in the membrane structure and MOF [34, 47, 48]. Fig. 5.c illustrates the permeation results of different gases from the PEBA1657MIL-100 (Fe) and PEBA2533/MIL-100 (Fe). As observed, CO<sub>2</sub> has scored more permeability in all parentages. The permeations are as below:



The rubber nature of PEBA makes the more polar nature of CO<sub>2</sub> more permeable than other gases. On the other hand, the kinetic diameter of CO<sub>2</sub> is smaller than O<sub>2</sub>, N<sub>2</sub> and CH<sub>4</sub>. It may be directed into more

permeation of this gas in comparison with other gases [31, 47]. Moreover, the weak solubility of  $N_2$  may be caused by the low permeability of the more kinetic diameter. Finally, it leads to less permeation. The permeation- dissolution mechanism has been widely accepted in order to explain the permeation of gases through the polymeric membranes. It is noteworthy that the principle of this mechanism is based on the gas transition through MIL-100 (Fe) caused by the simultaneous impact of the factors of MOF percentage compound, the size and structure of pores. MIL-100 has suitable molecular screening effects for the sake of engineered crystalline structures and the size of pores. In fact, the permeability of gases is enhanced by adding MIL-100 (Fe) to the structure of both PEBAX grades [50, 51].

Figure 6 discloses the effect of adding different percentages of MOF to the PEBAX structure on the separation operation of the synthesized membranes at the pressure of 5.5 bar. Figure 6.a. divulges that the permeation of carbon dioxide has been increased for both membranes with the PEBAX base as the MOF amount enhanced at the pressure of 5.5 bar. Besides, it is observed that the trend of changes at the pressure of 5.45 bar is similar to the tests done at the pressure of 3.5 bar. However, both permeability and selectivity have been enhanced to higher amounts. In other words, as the pressure is increased from 3.5 bar to 5.5 bar, the PEBAX1657/MIL-100 (Fe) membrane has reflected better operation than PEBAX2533/MIL-100 (Fe) in the separation of the tested gases. This phenomenon is caused by higher FFV of PEBAX2533/MIL-100 (Fe) membranes which are dense by pressure increase. As a result, the gas permeation coefficient is reduced in polymer due to the ( $D=A\exp(-\gamma v^*/FFV)$  Cohen-Turnbull)).

It is observed that the highest separation amount and ideal selectivity were observed in membranes with a loading of 5 wt.% of MOF. This phenomenon is brought about by MIL-100 (Fe) lumping in the mixed matrix membrane [47].

### 3-3. Comparison of the Permeability and Selectivity results of Prepared MMM

The graphs of 1991 [24] and 2008 [25] were used in order to scrutinize the separation operation of the synthesized membranes with other mixed matrix membranes and nanocomposite. These graphs have been achieved based on the selectivity and permeability data of the certain number of gases in previous studies designed by Robeson. These graphs have been considered as an operational criterion in lots of research on the membrane gaseous separation. In fact, if the operation of a membrane touches the graph or passes through it, its operation is acceptable [34, 47]. The graphs of Fig. 6 indicated that the operation of PEBAX1657/MIL-100 (Fe) membrane on the Robeson graph of 1991 is associated with  $CO_2/CH_4$  separation and PEBAX2533/MIL-100 (Fe) has touched it. The function of the synthesized membranes is respectively lower than Robeson graphs of 1991 and 2008 in the separation of the  $CO_2/N_2$  and  $O_2/N_2$  pair gases. It means that the PEBAX1657/MIL-100 (Fe) membrane has a relatively suitable operation to separate methane and carbon dioxide gases. The gradual increase of permeation by pressure enhancement is attributed to increasing the absorption of  $CO_2$  in the polymeric membranes [51].

Likewise, one the reasons of improving the operation of  $CO_2$  by pressure enhancement is caused by making hydrogen bonds among oxygen atoms existing in  $CO_2$  and Amide operational groups in PEBAX.

In fact, the permeation of CO<sub>2</sub> in PEBA2533-MIL-100 (Fe) is improved more than PEBA1657-MIL-100 (Fe) (Fig. 6.c). Additionally, more permeation of carbon dioxide might be related to enhancing the permeability of CO<sub>2</sub> in the mixed matrix membranes in comparison with other gases. The main reason is that since there are OH bonds in the structure of MIL-100(Fe), CO<sub>2</sub> tends to pass through the MOF pores more than other gases.

## 4. Conclusions

Both types of membranes based on PEBA with different grades and loading percentage of MOF were dissected and observed with the contribution of the XRD experiment of the amorphous (polyamide) and crystalline phases (polyether oxide and polytetra ethylene oxide). Moreover, two sharp peaks at 5.56 and 11.05° proved the presence of MOF. According to the SEM results, it was observed that membranes synthesized based on the PEBA2533 hold more porous structure in comparison with the ones synthesized based on PEBA1657. Evidently, adding MIL-100 (Fe) to PEBA makes more roughness on the membrane surface. Additionally, it was observed that as this MOF is increased, the lumping amount is enhanced. Eventually, it brings about non-selective masses on the surface and membrane structure. The outcomes of permeability and selectivity experiments demonstrated that carbon dioxide has the highest amount of permeability, whereas N<sub>2</sub> gas revealed the least amount of permeability through the synthesized membranes for the sake of more chemical tendency to the membrane surface and the small kinetic diameter. The permeability of methane gas was more than oxygen gas. Moreover, the synthesized membranes based on PEBA2533 have revealed more permeability, whereas membranes containing PEBA1657 reflected better selectivity. Adding MIL-100 (Fe) to the membrane structure caused to improve separation and permeation of all the intended gases, while the enhancement of this substance decreased the selectivity of the paired gases despite the permeability increase. This is concluded by lumping MOFs on the surface and the structure of the synthesized membranes. As the operating pressure is increased to 5.5 bar, the improvement of the separation operation was observed in all data. The results comparing with Robeson diagrams indicated that PEBA1657/MIL-100 (Fe) and PEBA2533/MIL-100 (Fe) membranes contain 5 wt.% of MOF, which has a suitable operation in separating methane gas from carbon dioxide for the sake of the Robeson graph of 1991. However, their operation needs more modifications to separate other aforementioned gases.

## Declarations

**Conflict of interest:** the authors declare that they have no conflict of interest

## References

1. *Abd El Salam, H. M., Nassar, H. N., Khidr, A. S., & Zaki, T. (2018). Antimicrobial activities of green synthesized Ag nanoparticles@ Ni-MOF nanosheets. Journal of Inorganic and Organometallic Polymers and Materials, 28(6), 2791-2798.*

2. Wei, D., Xin, Y., Rong, Y., Li, Y., Zhang, C., Chen, Q., ... & Hao, Y. (2020). A Mesoporous Gd-MOF with Lewis Basic Sites for 5-Fu Delivery and Inhibition of Human Lung Cancer Cells In Vivo and In Vitro. *Journal of Inorganic and Organometallic Polymers and Materials*, 30(4), 1121-1131.
3. Sacourbaravi, R., Ansari-Asl, Z., Kooti, M., Nobakht, V., & Darabpour, E. (2020). Fabrication of Ag NPs/Zn-MOF Nanocomposites and Their Application as Antibacterial Agents. *Journal of Inorganic and Organometallic Polymers and Materials*, 30(11), 4615-4621.
4. Yekta, S., & Sadeghi, M. (2018). Investigation of the Sr 2+ Ions Removal from Contaminated Drinking Water Using Novel CaO NPs@ MOF-5 Composite Adsorbent. *Journal of Inorganic and Organometallic Polymers and Materials*, 28(3), 1049-1064.
5. Uflyand, I. E., Zhinzhiro, V. A., & Bryantseva, J. D. (2021). Synthesis and Study of Sorption, Antioxidant and Antibacterial Properties of MOF based on Cobalt Terephthalate and 1, 10-Phenanthroline. *Journal of Inorganic and Organometallic Polymers and Materials*, 1-12.
6. Saeedi Dehaghani, A. H., & Pirouzfard, V. (2017). Preparation of High-Performance Membranes Derived from Poly (4-methyl-1-pentene)/Zinc Oxide Particles. *Chemical Engineering & Technology*, 40(9), 1693-1701.
7. Behnia, N., & Pirouzfard, V. (2018). Effect of operating pressure and pyrolysis conditions on the performance of carbon membranes for CO<sub>2</sub>/CH<sub>4</sub> and O<sub>2</sub>/N<sub>2</sub> separation derived from polybenzimidazole/Matrimid and UIP-S precursor blends. *Polymer Bulletin*, 75(10), 4341-4358.
8. Hosseini, S. M., Pirouzfard, V., & Azami, H. (2017). The Influence of Synthesis Parameters on Vertically Aligned CNT Sheets: Empirical Modeling and Process Optimization Using Response Surface Methodology. *The Journal of membrane biology*, 250(6), 651-661.
9. Sarmadi, R., Salimi, M., & Pirouzfard, V. (2020). The assessment of honeycomb structure UiO-66 and amino functionalized UiO-66 metal-organic frameworks to modify the morphology and performance of Pebax® 1657-based gas separation membranes for CO<sub>2</sub> capture applications. *Environmental Science and Pollution Research*, 27(32), 40618-40632.
10. Sohrabi, N., Alihosseini, A., Pirouzfard, V., & Pedram, M. Z. (2020). Analysis of Dynamics Targeting CNT-Based Drug Delivery through Lung Cancer Cells: Design, Simulation, and Computational Approach. *Membranes*, 10(10), 283.
11. Saeedi Dehaghani, A. H., Pirouzfard, V., & Alihosseini, A. (2020). Novel nanocomposite membranes-derived poly (4-methyl-1-pentene)/functionalized titanium dioxide to improve the gases transport properties and separation performance. *Polymer Bulletin*, 77(12), 6467-6489.
12. Salimi, M., & Pirouzfard, V. (2018). Synthesis of a novel nano-ceramic membrane for hydrogen separation and purification. *Journal of the Australian Ceramic Society*, 54(2), 271-277.
13. Salimi, M., & Pirouzfard, V. (2018). Synthesis of a novel nano-ceramic membrane for hydrogen separation and purification. *Journal of the Australian Ceramic Society*, 1-7.
14. Dehaghani, A. H. S., Rashidian, S., Pirouzfard, V., & Su, C. H. (2021). The novel composite membranes containing chloride and acid functionalized multiwall carbon nanotube fillers for gas separation. *Colloid and Polymer Science*, 1-12.

15. Vahid Pirouzfard, Zarringhalam Moghaddam, A., and Mirza, B. (2012). *Physicochemical Properties and Combustion Performance of Gas Oil–Fuel Additives*. ASME. *Journal of energy resources technology*, 134(4): 041101.
16. Salimi, M., Pirouzfard, V., & Kianfar, E. (2017). *Novel nanocomposite membranes prepared with PVC/ABS and silica nanoparticles for C<sub>2</sub>H<sub>6</sub>/CH<sub>4</sub> separation*. *Polymer Science, Series A*, 59(4), 566-574.
17. Soleymanipour, S. F., Dehaghani, A. H. S., Pirouzfard, V., & Alihosseini, A. (2016). *The morphology and gas-separation performance of membranes comprising multiwalled carbon nanotubes/polysulfone–Kapton*. *Journal of Applied Polymer Science*, 133(34).
18. Kianfar, E., Pirouzfard, V., & Sakhaeinia, H. (2017). *An experimental study on absorption/stripping CO<sub>2</sub> using mono-ethanol amine hollow fiber membrane contactor*. *Journal of the Taiwan Institute of Chemical Engineers*, 80, 954-962.
19. Saeedi Dehaghani, A. H., & Pirouzfard, V. (2017). *Preparation of High-Performance Membranes Derived from Poly (4-methyl-1-pentene)/Zinc Oxide Particles*. *Chemical Engineering & Technology*, 40(9), 1693-1701.
20. Salimi, M., & Pirouzfard, V. (2018). *Preparation and characterization of a novel MMMs by comprising of PSF–HNT/TiO<sub>2</sub> nanotubes to reduce organic sediments*. *Polymer Bulletin*, 75(6), 2285-2299.
21. A.H.S. Dehaghani, Vahid Pirouzfard, A. Alihosseini (2019) *Novel Nano-composite membranes derived poly (4-methyl-1-Pantene) / functionalized titanium dioxide to improve the gases transport properties and separation performance*. *Polymer Bulletin*.
22. N.N. Li, A.G. Fane, W.S. Winston, T. Matsuura, *Advanced Membrane Technology and Applications*. Copyright, 2008 John Wiley & Sons, Inc.
23. E. Schindler, F.Maier, *Manufacture of porous carbon membranes*, US patent 4919860, 1990.
24. Lloyd M. Robeson, *Correlation of separation factor versus permeability for polymeric membranes*, *Journal of Membrane Science*, Volume 62, Issue 2, 1991, Pages 165-185.
25. Lloyd M. Robeson, *The upper bound revisited*, *Journal of Membrane Science*, Volume 320, Issues 1–2, 2008, Pages 390-400,
26. De Q Vu, William J Koros, Stephen J Miller, *Mixed matrix membranes using carbon molecular sieves: I. Preparation and experimental results*, *Journal of Membrane Science*, Volume 211, Issue 2, 2003, Pages 311-334.
27. Jianhua Zhao, Ke Xie, Liang Liu, Min Liu, Wenlian Qiu, Paul A. Webley, *Enhancing plasticization-resistance of mixed-matrix membranes with exceptionally high CO<sub>2</sub>/CH<sub>4</sub> selectivity through incorporating ZSM-25 zeolite*, *Journal of Membrane Science*, Volume 583, 2019, Pages 23-30
28. Chen, M.-L., S.-Y. Zhou, Z. Xu, L. Ding and Y.-H. Cheng, *Metal-Organic Frameworks of MIL-100 (Fe, Cr) and MIL-101 (Cr) for Aromatic Amines Adsorption from Aqueous Solutions*. *Molecules*, 2019. 24(20): p. 3718.
29. Fu, Y.-Y., C.-X. Yang and X.-P. Yan, *Metal-organic framework MIL-100 (Fe) as the stationary phase for both normal-phase and reverse-phase high performance liquid chromatography*. *Journal of*

- Chromatography A*, 2013. 1274: p. 137-144.
30. Wang, X., et al., *Highly dispersible and stable copper terephthalate metal-organic framework-graphene oxide nanocomposite for an electrochemical sensing application. ACS applied materials & interfaces*, 2014. 6(14): p. 11573-11580.
  31. Murali, R.S., S. Sridhar, T. Sankarshana and Y. Ravikumar, *Gas permeation behavior of PEBA-X-1657 nanocomposite membrane incorporated with multiwalled carbon nanotubes. Industrial & Engineering Chemistry Research*, 2010. 49(14): p. 6530-6538.
  32. Lun Shu, Lin-Hua Xie, Yingshuang Meng, Tongxin Liu, Cui Zhao, Jian-Rong Li, *A thin and high loading two-dimensional MOF nanosheet based mixed-matrix membrane for high permeance nanofiltration, Journal of Membrane Science*, Volume 603, 2020, 118049.
  33. Heng Mao, Shen-Hui Li, Ao-Shuai Zhang, Li-Hao Xu, Jiao-Jiao Lu, Zhi-Ping Zhao, *Novel MOF-capped halloysite nanotubes/PDMS mixed matrix membranes for enhanced n-butanol permselective pervaporation, Journal of Membrane Science*, Volume 595, 2020, 117543.
  34. Azizi, N. and M.M. Zarei, *CO<sub>2</sub>/CH<sub>4</sub> separation using prepared and characterized poly (ether-block-amide)/ZIF-8 mixed matrix membranes. Petroleum Science and Technology*, 2017. 35(9): p. 869-874.
  35. Tiwari, B., B. Sellamuthu, Y. Ouarda, P. Drogui, R.D. Tyagi and G. Buelna, *Review on fate and mechanism of removal of pharmaceutical pollutants from wastewater using biological approach. Bioresource technology*, 2017. 224: p. 1-12.
  36. Mozafari, M., R. Abedini and A. Rahimpour, *Zr-MOFs-incorporated thin film nanocomposite PEBA-X-1657 membranes dip-coated on polymethylpentylene layer for efficient separation of CO<sub>2</sub>/CH<sub>4</sub>. Journal of Materials Chemistry A*, 2018. 6(26): p. 12380-12392.
  37. Rabiee, H., A. Ghadimi and S. Abbasi, *CO<sub>2</sub> separation performance of poly (ether-b-amide6)/PTMEG blended membranes: Permeation and sorption properties. Chemical Engineering Research and Design*, 201:98, 96-106.
  38. Nafisi, V. and M.-B. Hägg, *Development of dual layer of ZIF-8/PEBA-X-2533 mixed matrix membrane for CO<sub>2</sub> capture. Journal of Membrane Science*, 2014. 459: p. 244-255.
  39. Mulder, J., *Basic principles of membrane technology*. 2012: Springer Science & Business Media.
  40. Biswas, S. and P. Van Der Voort, *A general strategy for the synthesis of functionalised UiO-66 frameworks: characterisation, stability and CO<sub>2</sub> adsorption properties. European Journal of Inorganic Chemistry*, 2013. 2013(12): p2154-60
  41. Cmarik, G.E., M. Kim, S.M. Cohen and K.S. Walton, *Tuning the adsorption properties of UiO-66 via ligand functionalization. Langmuir*, 2012. 28(44): p. 15606-15613.
  42. Chen, J.C., X. Feng and A. Penlidis, *Gas Permeation Through Poly (Ether-b-amide)(PEBA-X-2533) Block Copolymer Membranes. Separation science and technology*, 2005. 39(1): p. 149-164.
  43. Sanaeepur, H., S. Mashhadikhan, G. Mardassi, A.E. Amooghin, B. Van der Bruggen and A. Moghadassi, *Aminosilane cross-linked poly ether-block-amide PEBA-X-2533: Characterization and CO<sub>2</sub> separation properties. Korean Journal of Chemical Engineering*, 2019. 36(8): p. 1339-1349.

44. Jomekian, A., R.M. Behbahani, T. Mohammadi and A. Kargari, High speed spin coating in fabrication of PEBA<sub>X</sub> 1657 based mixed matrix membrane filled with ultra-porous ZIF-8 particles for CO<sub>2</sub>/CH<sub>4</sub> separation. *Korean Journal of Chemical Engineering*, 2017. 34(2): p. 440-453.
45. Wang, S., Y. Liu, S. Huang, H. Wu, Y. Li, Z. Tian and Z. Jiang, PEBA<sub>X</sub>-PEG-MWCNT hybrid membranes with enhanced CO<sub>2</sub> capture properties. *Journal of membrane science*, 2014. 460: p. 62-70.
46. Yang, L., S. Zhang, H. Wu, C. Ye, X. Liang, S. Wang, X. Wu, Y. Wu, Y. Ren and Y. Liu, Porous organosilicon nanotubes in PEBA<sub>X</sub>-based mixed-matrix membranes for biogas purification. *Journal of membrane science*, 2019. 573: p. 301-308.
47. Isanejad, M. and T. Mohammadi, Effect of amine modification on morphology and performance of poly (ether-block-amide)/fumed silica nanocomposite membranes for CO<sub>2</sub>/CH<sub>4</sub> separation. *Materials Chemistry and Physics*, 2018. 205: p. 303-314.
48. Ahmadpour, E., A.A. Shamsabadi, R.M. Behbahani, M. Aghajani and A. Kargari, Study of CO<sub>2</sub> separation with PVC/PEBA<sub>X</sub> composite membrane. *Journal of Natural Gas Science and Engineering*, 2014. 21: p. 518-23.
49. Sridhar, S., R. Suryamurali, B. Smitha and T. Aminabhavi, Development of crosslinked poly (ether-block-amide) membrane for CO<sub>2</sub>/CH<sub>4</sub> separation. *Colloids and Surfaces A: Physicochemical and Engineering Aspects*, 2007. 297(1-3): p. 267-274.
50. Horcajada, P., S. Surblé, C. Serre, D.-Y. Hong, Y.-K. Seo, J.-S. Chang, J.-M. Greneche, I. Margiolaki and G. Férey, Synthesis and catalytic properties of MIL-100 (Fe), an iron (III) carboxylate with large pores. *Chemical Communications*, 2007(27): p. 2820-2822.
51. Dong, G., J. Hou, J. Wang, Y. Zhang, V. Chen and J. Liu, Enhanced CO<sub>2</sub>/N<sub>2</sub> separation by porous reduced graphene oxide/PEBA<sub>X</sub> mixed matrix membranes. *Journal of Membrane Science*, 2016. 520: p. 860-868.

## Figures

(a)



(b)



**Figure 1**

The (a) membrane preparation setup and (b) membrane module

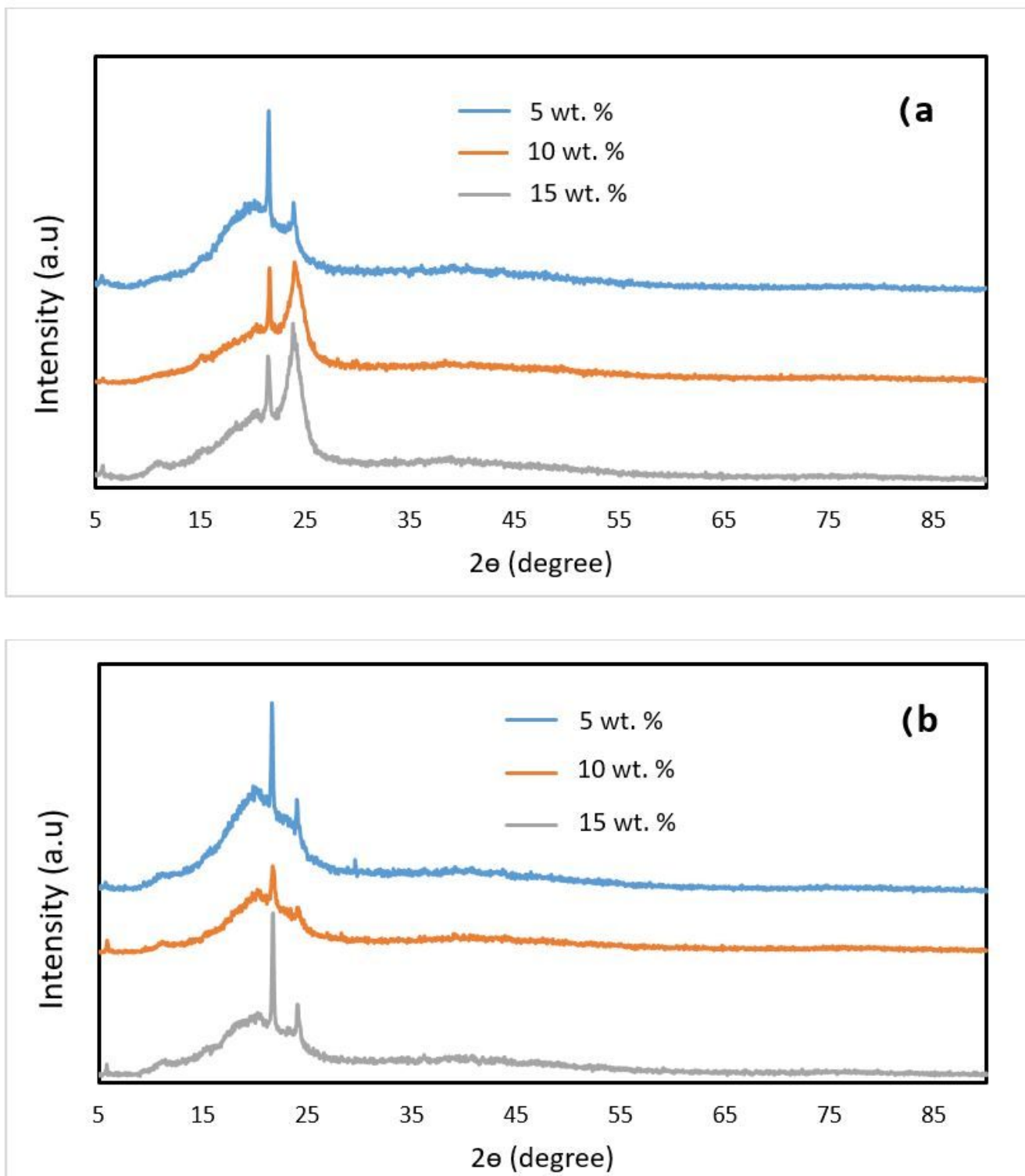


**Figure 2**

X-ray diffraction test results for (a) PEBA1657 / MIL-100 (Fe) and (b) PEBA2533 / MIL-100 (Fe) membranes with various loading percentage.

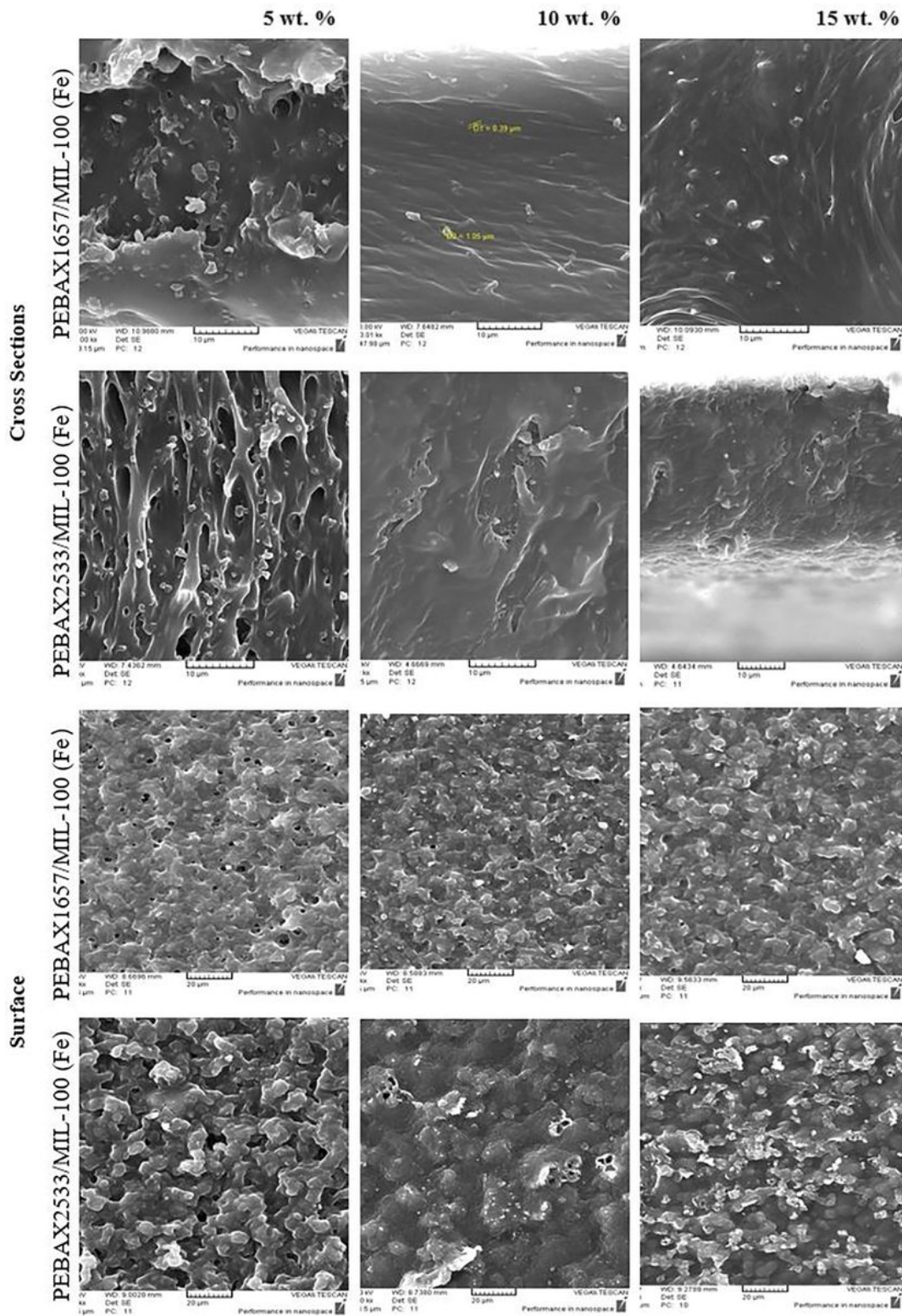


**Figure 3**

SEM photographs of the surface and cross sections of the PEBAX1657 / MIL-100 (Fe) and PEBAX2533 / MIL-100 (Fe) nanocomposite membranes in various loading percentage

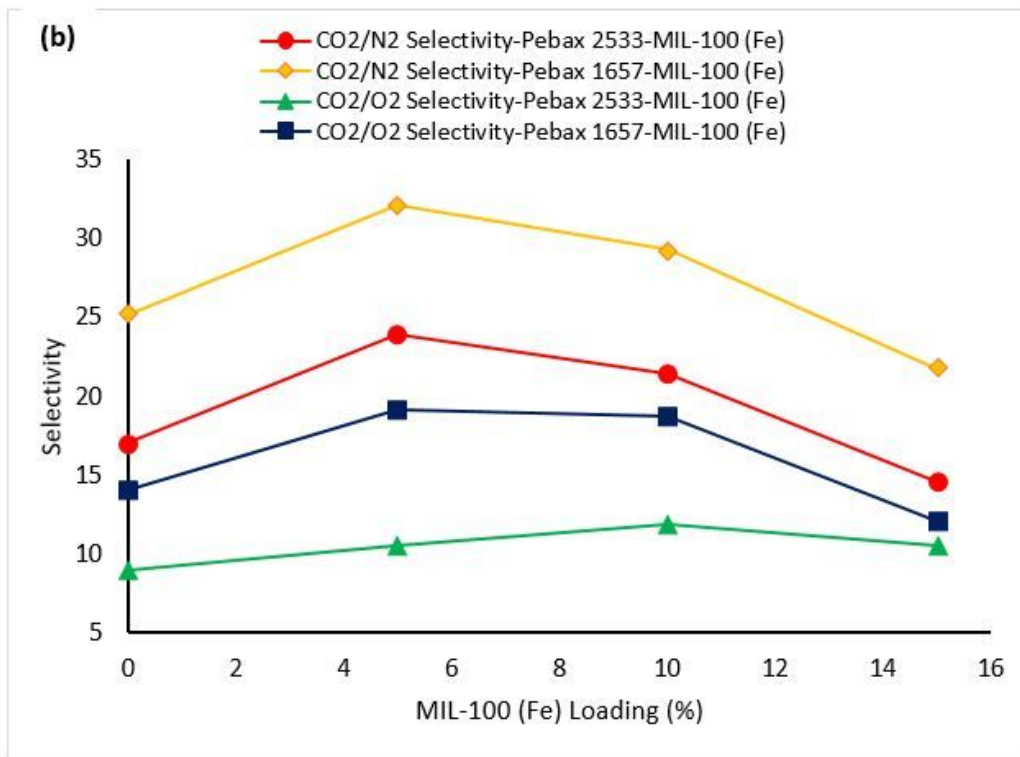
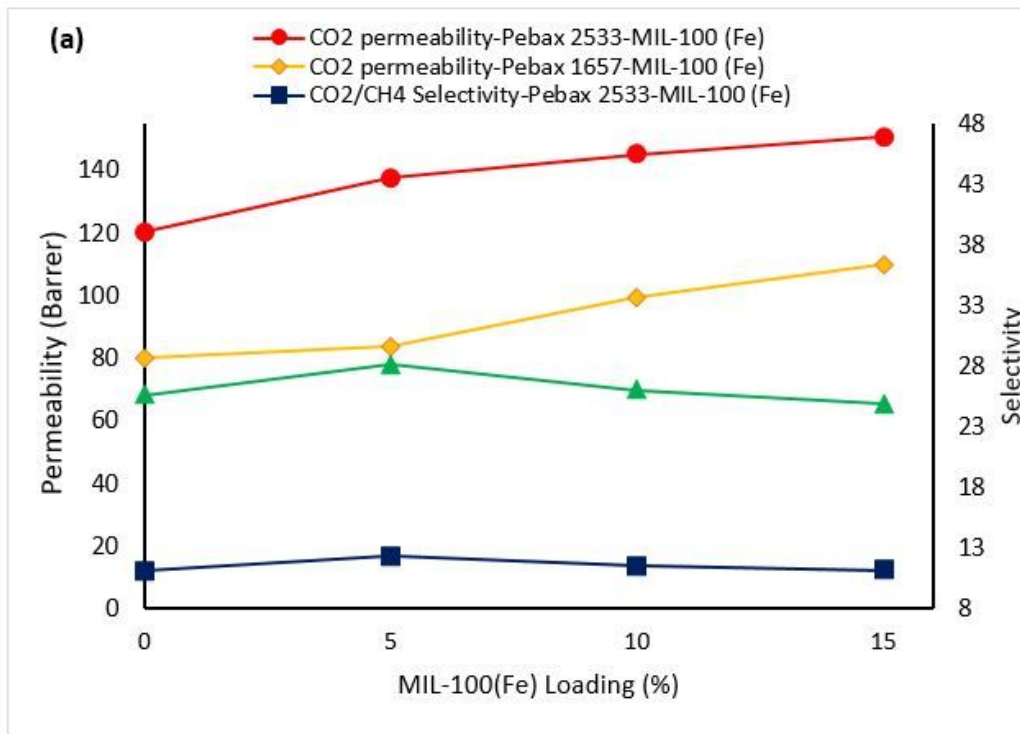


**Figure 4**

Comparison of the separation performance of PEBAX1657 / MIL-100 (Fe) and PEBAX2533 / MIL-100 (Fe) membranes due to increasing MIL-100 (Fe) loading percentages; (a) CO<sub>2</sub> permeability and (b) gas pair selectivity of CO<sub>2</sub>/N<sub>2</sub> and CO<sub>2</sub>/O<sub>2</sub> at pressure of 3.5 bar.

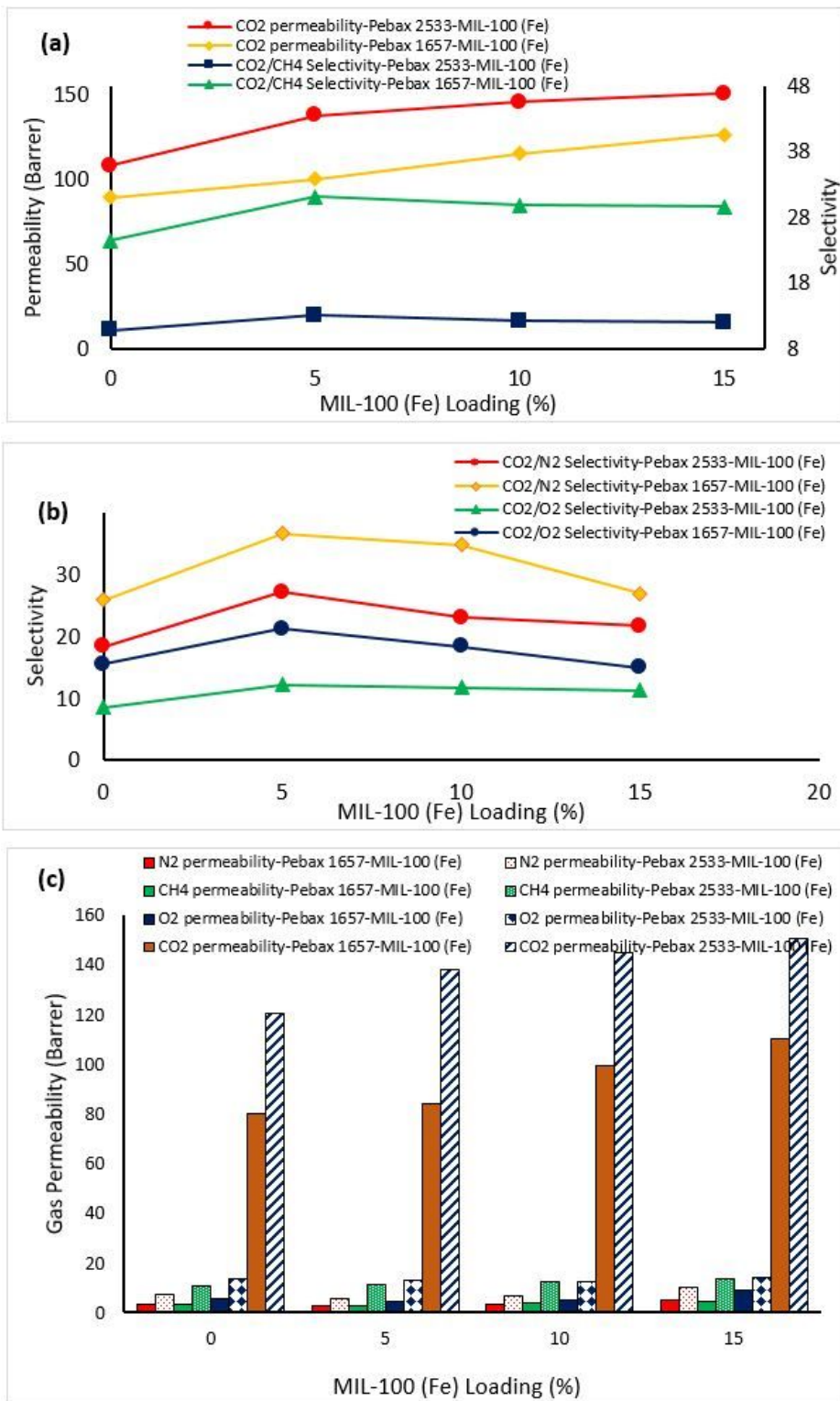


**Figure 5**

Comparison of the separation performance of PEBAX1657 / MIL-100 (Fe) and PEBAX2533 / MIL-100 (Fe) membranes due to increasing loading percentages of MIL-100 (Fe); (a) CO<sub>2</sub> permeability and CO<sub>2</sub>/CH<sub>4</sub> selectivity at pressure of 5.5 bar (b) selectivity of CO<sub>2</sub>/N<sub>2</sub> and CO<sub>2</sub>/O<sub>2</sub> at pressure of 5.5 bar. (c) Permeability of CO<sub>2</sub>, CH<sub>4</sub>, N<sub>2</sub> and O<sub>2</sub> at a pressure of 3.5 bar.

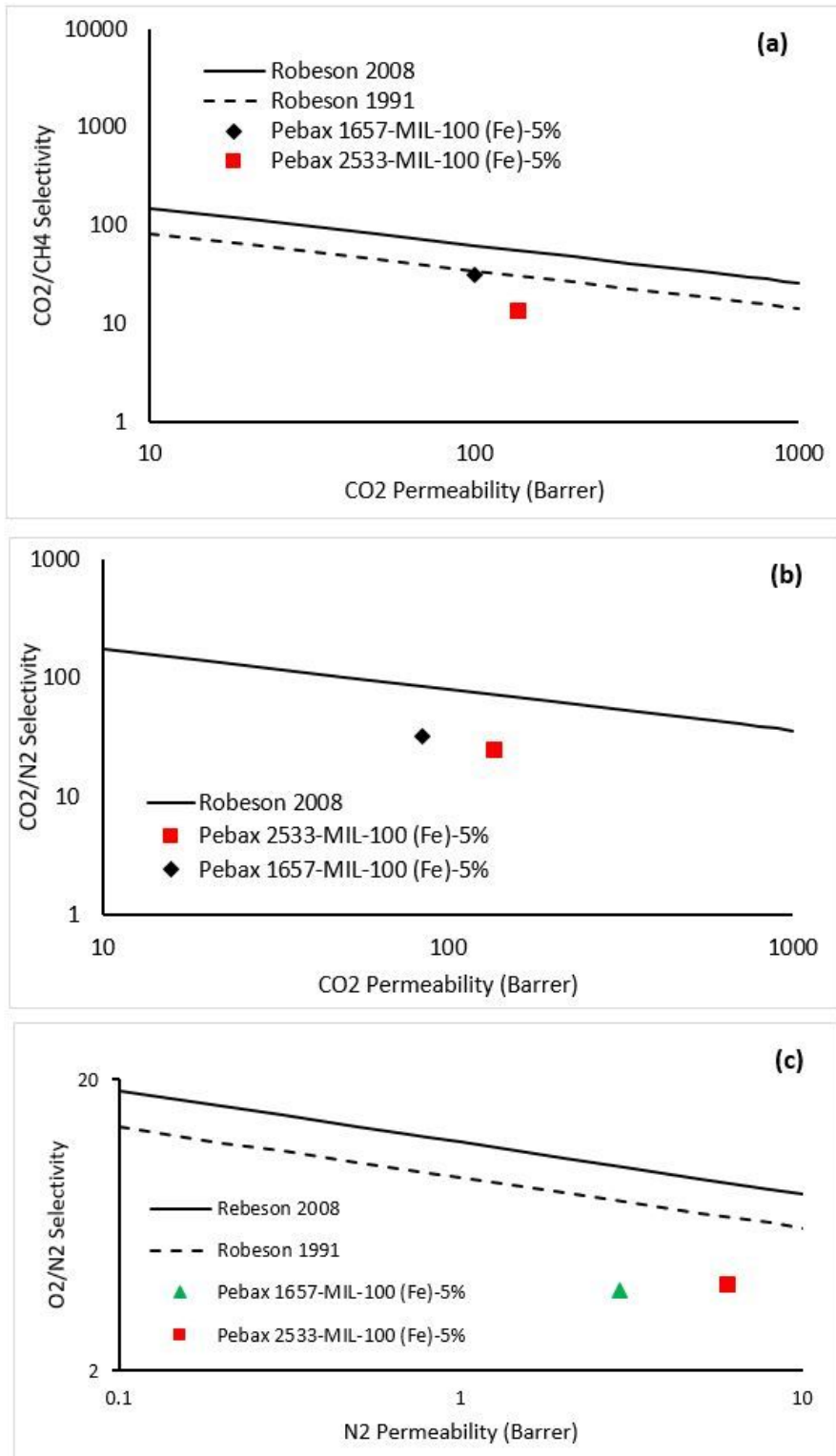


**Figure 6**

Separation performance of PEBAx1657 / MIL-100 (Fe) and PEBAx2533 / MIL-100 (Fe) membranes in compared with Robson diagrams for (a) CO<sub>2</sub>/CH<sub>4</sub> (b) CO<sub>2</sub>/N<sub>2</sub> and (c) O<sub>2</sub>/N<sub>2</sub>